DOI: 10.1002/chem.200701725

Mechanism, Regioselectivity, and the Kinetics of Phosphine-Catalyzed [3+2] Cycloaddition Reactions of Allenoates and Electron-Deficient Alkenes

Yong Liang,[a] Song Liu,[a] Yuanzhi Xia,[a, b] Yahong Li,[b, c] and Zhi-Xiang Yu*[a]

Abstract: With the aid of computations and experiments, the detailed mechanism of the phosphine-catalyzed [3+2] cycloaddition reactions of allenoates and electron-deficient alkenes has been investigated. It was found that this reaction includes four consecutive processes: 1) In situ generation of a 1,3-dipole from allenoate and phosphine, 2) stepwise [3+2] cycloaddition, 3) a water-catalyzed [1,2]-hydrogen shift, and 4) elimination of the phosphine catalyst. In situ generation of the 1,3-dipole is key to all nucleophilic phosphine-catalyzed reactions. Through a kinetic study we have shown that the generation of the 1,3-dipole is the rate-determining step of the phosphine-catalyzed [3+2] cycloaddition reaction of allenoates and electron-deficient alkenes. DFT calculations and FMO analysis revealed that an electron-withdrawing group is required in the allene to ensure the generation of the 1,3-dipole kinetically and thermodynamically. Atoms-in-molecules (AIM) theory was used to analyze the stability of the 1,3-dipole. The regioselectivity of the [3+2] cycloaddition can be rationalized very well by FMO and AIM theories. Isotopic labeling experiments combined with DFT calculations showed that the commonly accepted intramolecular [1,2]-proton shift should be corrected to a water-catalyzed [1,2]-proton shift. Additional isotopic labeling experiments of the hetero-[3+2] cycloaddition of allenoates and electron-deficient imines further support this finding. This investigation has also been extended to the study of the phosphine-catalyzed [3+2] cycloaddition reaction of alkynoates as the three-carbon synthon, which showed that the generation of the 1,3-dipole in this reaction also occurs by a water-catalyzed process.

Keywords: allenes · density functional calculations · kinetics · phosphine organocatalysis · reaction mechanisms

Introduction

The Huisgen [3+2] cycloaddition reactions between 1,3-dipoles and dipolarophiles have been widely applied in the construction of five-membered heterocycles.[1,2] Inspired by the success of Huisgen's chemistry and other cycloaddition reactions such as the Diels–Alder reaction, which has been widely employed in the synthesis of six-membered carbocycles and heterocycles, synthetic chemists have been continuously searching for analogous [3+2] cycloaddition reactions to synthesize five-membered carbocycles and heterocycles, which exist predominantly as the backbones of many natural products and other compounds of pharmaceutical significance. Endeavors in this line have led to the discoveries of several elegant [3+2] cycloaddition reactions by Danheiser,[3] Trost,[4] Lu,[5] and others.[6] All these [3+2] cycloaddition reactions employ Lewis acids or transition metals as catalysts with the exception of Lu's [3+2] cycloaddition reactions of allenoates and electron-deficient alkenes or imines which occur by catalysis with tertiary phosphines (Scheme 1). This reaction can also be executed by using alkynoates instead of allenoates as the three-carbon synthon (Scheme 1). Because phosphines are organocatalysts, Lu's [3+2] cycloaddition reaction can be regarded as one of the recently widely pursued organocatalytic reactions.[7] Lu, Kri-

[a] Y. Liang, S. Liu, Y. Xia, Prof. Dr. Z.-X. Yu
Beijing National Laboratory for Molecular Sciences (BNLMS)
Key Laboratory of Bioorganic Chemistry and Molecular Engineering of the Ministry of Education, College of Chemistry
Peking University
Beijing 100871 (China)
Fax: (+86) 10-6275-1708
E-mail: yuzx@pku.edu.cn

[b] Y. Xia, Prof. Dr. Y. Li
Qinghai Institute of Salt Lakes, Chinese Academy of Sciences
Xining 810008 (China)

[c] Prof. Dr. Y. Li
Key Laboratory of Organic Synthesis of Jiangsu Province
Department of Chemistry and Chemical Engineering
Suzhou University
Suzhou 215006 (China)

Supporting Information for this article is available on the WWW under http://www.chemeurj.org/ or from the author.

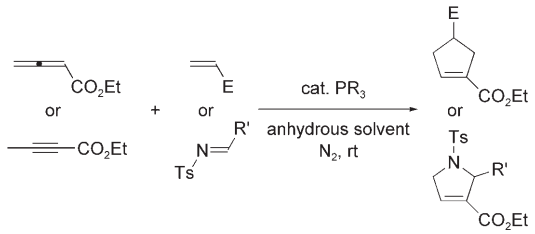

Scheme 1. The phosphine-catalyzed [3+2] cycloaddition reaction (only the major product is given; E = electron-withdrawing group).

sche, and Pyne and their co-workers have used this [3+2] cycloaddition reaction as a key step in the total synthesis of natural products.[5c,8] As a result of studies by Zhang, Fu, and Miller and their co-workers, asymmetric versions of phosphine-catalyzed [3+2] cycloaddition reactions have also been developed.[9] Since the discovery of the phosphine-catalyzed [3+2] cycloaddition reaction in 1995,[5a] further elegant developments and extensions of the chemistry based on nucleophilic phosphine catalysis have been widely pursued by many other groups[10] and this chemistry is enriching the arsenal of chemical reactions.[11]

The commonly accepted mechanism for the phosphine-catalyzed [3+2] cycloaddition reaction of allenoates and activated alkenes is given in Scheme 2.[5a,11a] The catalytic cycle

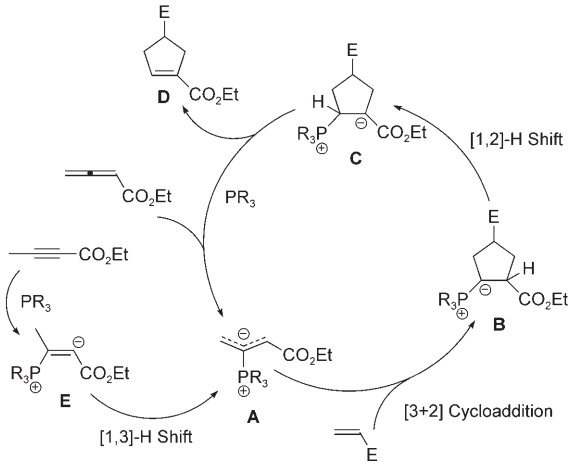

Scheme 2. The mechanisms originally proposed for the phosphine-catalyzed [3+2] cycloaddition reactions (only the major product is given; E = electron-withdrawing group).

starts with the formation of a zwitterionic intermediate **A**, generated from allenoate and phosphine, which acts as a 1,3-dipole, reacting with an electron-deficient alkene to give five-membered phosphorus ylide **B**. Then a [1,2]-proton shift converts **B** into another zwitterionic intermediate **C**, which gives rise to the final product **D** by elimination of the phosphine catalyst. The phosphine-catalyzed [3+2] cycloaddition reaction between alkynoates and dipolarophiles also has to occur via zwitterionic intermediate **A** to enter into the [3+2] catalytic cycle. In this case, it was proposed that zwitterionic intermediate **A** was formed by a [1,3]-proton shift in zwitterionic intermediate **E** generated from the alkynoate and phosphine (Scheme 2).[5a]

Despite the widespread application of phosphine-catalyzed [3+2] cycloaddition reactions and the continuing development of phosphine-catalyzed organocatalysis[10,11] and allene chemistry,[12] the detailed mechanism of phosphine-catalyzed [3+2] cycloaddition reactions has not been investigated experimentally or theoretically. To the best of our knowledge only a few studies have been conducted to rationalize the regioselectivity of these reactions by scrutinizing the [3+2] cycloaddition transition-state structures located by theoretical calculations.[13] The originally proposed [1,2]-proton shift had not been investigated experimentally or computationally until we published our preliminary results.[14] Furthermore, no detailed studies of the overall process of phosphine-catalyzed [3+2] cycloaddition reactions have been documented. Kinetic information on the [3+2] cycloaddition reaction has not been obtained either. In addition, it is still unclear how 1,3-dipoles are generated from alkynoates and phosphine.

Herein we disclose the detailed mechanism of the phosphine-catalyzed [3+2] cycloaddition reaction through joint computational and experimental studies with an emphasis on how the 1,3-dipoles are generated, the geometric features of the 1,3-dipoles, and how water and other protic solvents catalyze this reaction. We have also carried out kinetic studies to quantitatively analyze the phosphine-catalyzed [3+2] cycloaddition reaction of allenoates and electron-deficient alkenes. These mechanistic studies give an insight into the chemistry of nucleophilic phosphine organocatalysis and related reactions in general.[10] In addition, these mechanistic insights will act as a guide in the future design of new reactions and new chiral organocatalysts. Furthermore, the results of this study will prompt chemists to rethink the role of a trace amount of water in "anhydrous" organic reactions that involve [1,*n*]-hydrogen shifts.[10]

Computational Methods

All of the DFT calculations were performed with the Gaussian 03 software package.[15] Geometry optimization of all the minima and transition states involved was carried out at the B3LYP level of theory[16] with the 6-31+G(d) basis set.[17] A diffuse function in the basis set is important to describe zwitterionic species.[18] The vibrational frequencies were computed at the same level of theory to check whether each optimized structure is an energy minimum or a transition state and to evaluate its zero-point vibrational energy (ZPVE). IRC calculations[19] were used to confirm that the transition states connect the corresponding reactants and products. Solvent effects were computed using the CPCM model[20] at the B3LYP/6-31+G(d) level of theory using the gas-phase-optimized structures. The natural bond orbital (NBO) technique[21] was applied to calculate the Wiberg bond indices to analyze the bonding. Topological analysis of the electron densities at bond critical points was performed with the AIM 2000 program.[22]

Results and Discussion

Generation of the 1,3-dipole from allenoate: The first step in the phosphine-catalyzed [3+2] cycloaddition of an allenoate and alkene is the nucleophilic attack of the phosphine catalyst on the allenoate to generate in situ a zwitterionic intermediate, which serves as a 1,3-dipole. This step is key to all reactions involving allenes and nucleophilic phosphine catalysts.[10] The kinetic and thermodynamic parameters of this process have been computed. Figure 1 shows the energy surfaces computed for the addition of trimethylphosphine (**2**) to methyl 2,3-butadienoate (**1**) and the parent allene (**1′**). The addition of phosphine to **1′** was studied in order to understand substituent effects in allenes. The optimized structures are shown in Figure 2.

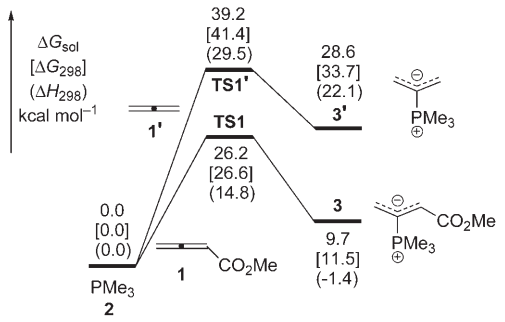

Figure 1. DFT-computed energy surfaces for the reactions between **1/1′** and **2**.

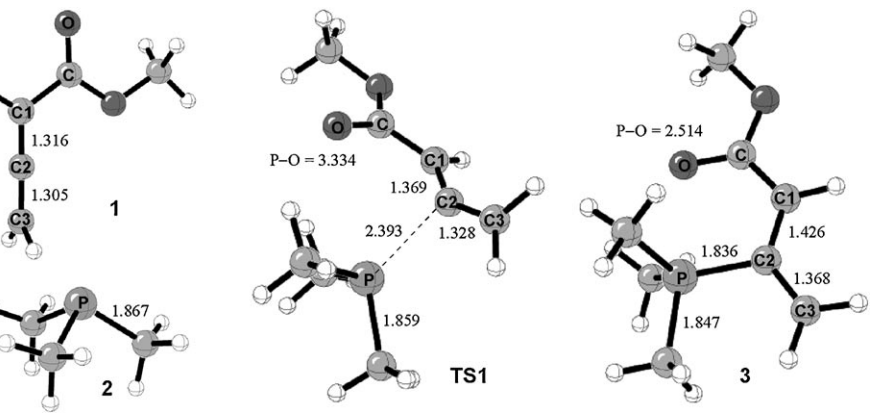

Figure 2. DFT-optimized structures of **1**, **2**, transition state **TS1**, and 1,3-dipole **3**. Distances are in Å.

Calculations indicate that, in the gas phase, the formation of the zwitterionic 1,3-dipole **3** is exothermic by 1.4 kcal mol^{-1} in terms of enthalpy, but is endergonic by 9.7 kcal mol^{-1} owing to entropy loss. The activation enthalpy for this nucleophilic addition is 14.8 kcal mol^{-1} and its activation free energy is 26.6 kcal mol^{-1} in the gas phase.[23] After taking solvent effects into consideration, the computed activation free energy is 26.2 kcal mol^{-1} in benzene (this value is overestimated as a result of an overestimation of the entropy in calculations, see later discussions on the reaction kinetics).

The forming C–P bond length in the addition transition-state structure **TS1** is 2.393 Å and the P-C2-C1-C dihedral angle is 57.9° (the atom numbering is given in Figure 2). To better understand this nucleophilic attack, we carried out a frontier molecular orbital (FMO) analysis[24] (Figure 3). The

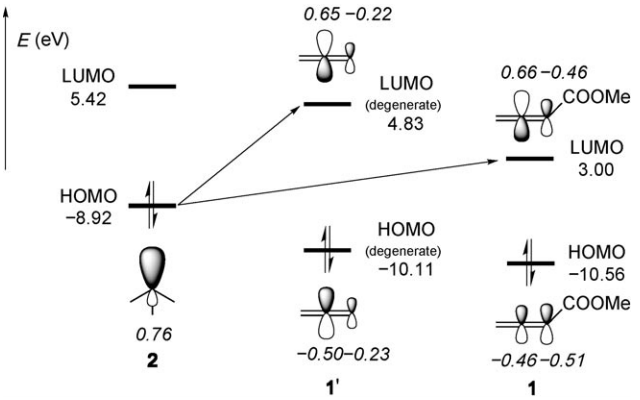

Figure 3. FMO diagram for the reactions between **1/1′** and **2**. Orbital coefficients are given in italics.[25]

energy gap of $HOMO_2$–$LUMO_1$ is much smaller than that of $HOMO_1$–$LUMO_2$ (11.92 versus 15.98 eV), which indicates that the major interaction in the transition state **TS1** is that between the phosphine's lone pair and the π* orbital of the C1=C2 double bond in **1**. This is the reason why phosphine attacks the C1=C2 double bond in a near perpendicular fashion in **TS1**.

The phosphine-catalyzed [3+2] cycloaddition reactions of allenes and alkenes are usually limited to allenes activated with strong electron-withdrawing groups. This can be easily appreciated by comparing the addition of phosphine to **1′**. The activation enthalpy and free energy in the gas phase for the addition of phosphine to **1′** are 29.5 and 41.4 kcal mol^{-1}, respectively. Both are about 15 kcal mol^{-1} higher than their counterparts in the addition of phosphine to **1**, which confirms that without an electron-withdrawing group on the allene, formation of the 1,3-dipole is kinetically disfavored. The lower reactivity of **1′** compared with **1** can be easily rationalized by FMO theory: The LUMO of **1′** is higher than that of **1** by 1.83 eV (the difference in energy between the HOMOs of **1** and **1′** is just 0.45 eV). Moreover, the forma-

tion of the 1,3-dipole **3′** is thermodynamically disfavored in terms of enthalpy as a result of an endothermicity of 22.1 kcal mol^{-1}. The above results show that the installation of an electron-withdrawing group in allene stabilizes both the transition state of phosphine addition and the 1,3-dipole formed.

Very recently, Kwon and co-workers obtained the crystal structures of stable tetravalent phosphonium enolate zwitterions.[26] The 1,3-dipole **3** can be regarded as a relatively less stable tetravalent phosphonium enolate zwitterion. Therefore, it is worth discussing the structure of the 1,3-dipole **3** shown in Figure 2. In theory, there are four possible structures for the 1,3-dipole generated from allenoate and phosphine (Figure 4). It was found that the most stable

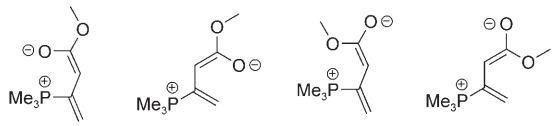

Figure 4. DFT-computed relative enthalpies and free energies of four possible structures of the 1,3-dipole generated from PMe_3 and allenoate.

structure for the 1,3-dipole is **3**. The formed P–C2 bond distance in **3** is 1.836 Å (Figure 2). More importantly, there is a short P–O distance (2.514 Å) between the phosphorus and carbonyl oxygen atoms. The Wiberg bond index shows the bond order between these two atoms is 0.10, which indicates that a significant intramolecular P···O interaction stabilizes this intermediate.[21] To better understand the energetic preference of **3** over **3b**, which also has a P···O interaction, we carried out an atoms-in-molecules (AIM) analysis of these two species (Figure 5 and Table 1).

Table 1 summarizes the computed electron density values (ρ), the corresponding Laplacian values ($\nabla^2\rho$), and the eigenvalues ($\lambda_1<\lambda_2<\lambda_3$, $\nabla^2\rho=\lambda_1+\lambda_2+\lambda_3$) for selected bond critical points. As shown in Figure 5, no bond critical point can be found between the oxygen and hydrogen atoms in **3**,

Table 1. Electron density topological properties of selected (3,−1) critical points in **3** and **3b**.

Interaction	Distance [Å]	ρ	$\nabla^2\rho$	λ_1	λ_2	λ_3
P···O (**3**)	2.514	0.0330	0.0626	−0.0252	−0.0216	0.1094
P···O (**3b**)	2.961	0.0123	0.0040	−0.0065	−0.0038	0.0503
H1···O (**3b**)	2.281	0.0161	0.0544	−0.0174	−0.0140	0.0858
H2···O (**3b**)	2.255	0.0165	0.0569	−0.0180	−0.0145	0.0894

which indicates the absence of bifurcated hydrogen bonding in this intermediate. However, such an interaction was found in its isomer **3b** in which the methoxy group is orientated towards the phosphorus atom. The H1···O and H2···O interactions[27] in **3b** have electron density values of 0.0161 and 0.0165 a.u. and Laplacian values of 0.0544 and 0.0569 a.u., respectively, which are within the range of a normal hydrogen bond.[28] As confirmed by the electron density topological analysis, the P···O interaction in **3** is much stronger than that in **3b** because the electron density value of the former is much larger than that of the latter (0.0330 versus 0.0123 a.u.). Despite the bifurcated hydrogen bonding in **3b**, the P···O interaction is the dominant stabilizing effect in the 1,3-dipole, making **3** lower in Gibbs free energy than **3b** by 8.2 kcal mol^{-1} in the gas phase.

Regioselectivity of the [3+2] cycloaddition process: When an unsymmetrical alkene is used as a dipolarophile in the phosphine-catalyzed [3+2] cycloaddition reaction of allenoates, two cycloadducts can be obtained as regioisomers. The origin of the regioselectivity of this reaction was explored by computing the energy surface of the [3+2] cycloaddition process (Figure 6, the transition-state structures involved are given in Figure 7). Previous work revealed that the [3+2] cycloaddition reaction occurs by a stepwise process.[13,14,29] In the α-addition mode, the first transition state α-**TS2** requires an activation free energy of only 18.2 kcal mol^{-1} in benzene. The subsequent ring-closure transition state α-**TS3** is slightly higher in energy than α-**TS2** by 0.4 kcal mol^{-1}. In the γ-addition mode, the two terminal carbon atoms form a C–C single bond via γ-**TS2** with an energy barrier of 19.4 kcal mol^{-1} in benzene. The subsequent ring-closure transition state γ-**TS3** is lower in energy than γ-**TS2** by 3.5 kcal mol^{-1}. Based on the energy difference (18.6 kcal mol^{-1} for the α-addition mode versus 19.4 kcal mol^{-1} for the γ-addition mode), our B3LYP/6-31+G(d) calculations predict a 79:21 product ratio for α- versus γ-cycloaddition, close to the experimental ratio of 85:15.[5a]

As α-**TS2** and α-**TS3** are very similar in energy, the above α- versus γ-cycloaddition regioselectivity can be analyzed by

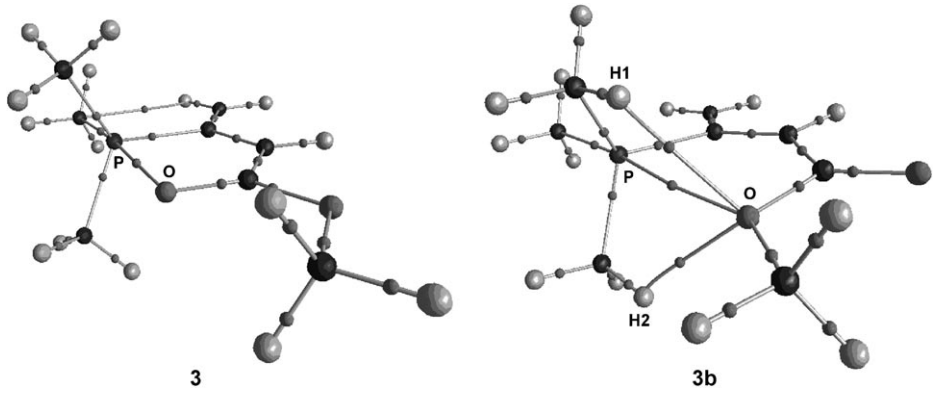

Figure 5. The bond critical points in the 1,3-dipole **3** and its isomer **3b**.

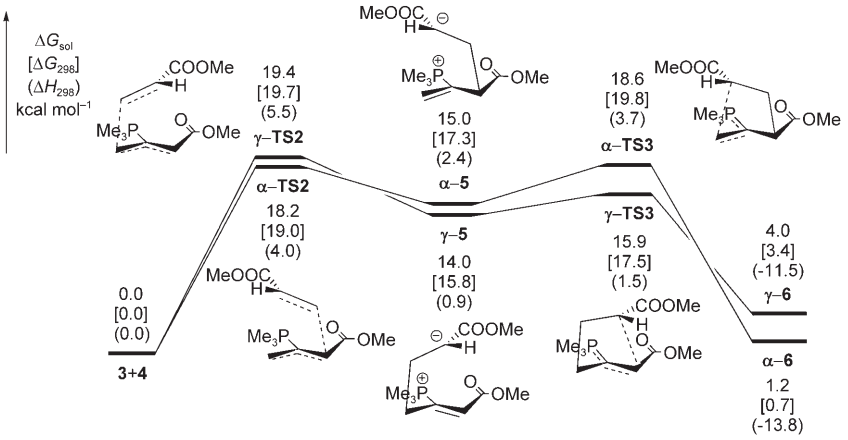

Figure 6. DFT-computed energy surfaces for the [3+2] cycloaddition of **3** and **4**.

comparing the relative energies of the Michael addition transition states α-**TS2** and γ-**TS2**. FMO theory[24,30] can be easily applied to explain why α-**TS2** is more favored than γ-**TS2** (Figure 8). The energy gap of the $HOMO_3$–$LUMO_4$ is much smaller than that of $HOMO_4$–$LUMO_3$ (9.15 versus 14.44 eV), which indicates that the most favored orbital interaction in the transition state is between the allylic anion fragment of the 1,3-dipole **3** and the π* orbital of the C=C bond in the acrylate **4**. The HOMO coefficient of C1 (the atom numbering is given in Figure 7 and Figure 8) in the 1,3-dipole **3** is larger than that of C3 (0.69 versus 0.55), which suggests that C1 rather than C3 is a better match with C4 (with a LUMO coefficient of 0.68, Figure 8) in **4**, according to FMO theory. Therefore, the [3+2] cycloaddition from C1 (the α position) of the 1,3-dipole **3** is more favored than that from C3 (the γ position).

In addition to the satisfactory explanation of the above regioselectivity by FMO theory, analysis of the structures of α-**TS2** and γ-**TS2** can also explain their relative stability.[31] Here we present our understanding of the structures of α-**TS2** and γ-**TS2** with the aid of AIM analysis. AIM analysis indicates that there is no P···O interaction between the phosphorus and the carbonyl oxygen atom of the alkenoate moiety (O2 in Figure 9) in either α-**TS2** or γ-**TS2**. The P···O1 interactions in α-**TS2** and γ-**TS2** (Table 2) are weaker than that in the 1,3-dipole **3** (Table 1) as their electron densities are much lower than that of **3** (0.0129 a.u. in α-**TS2**, 0.0145 a.u. in γ-**TS2**, 0.0330 a.u. in **3**). However, there are several hydrogen-bonding interactions in both α-**TS2** and γ-**TS2** (Figure 9). Compared with γ-**TS2**, α-**TS2** has one more hydrogen bond (H4···O2, Figure 9), although the other H···O and P···O interactions in it are all slightly weaker than those in γ-**TS2** (Table 2). This

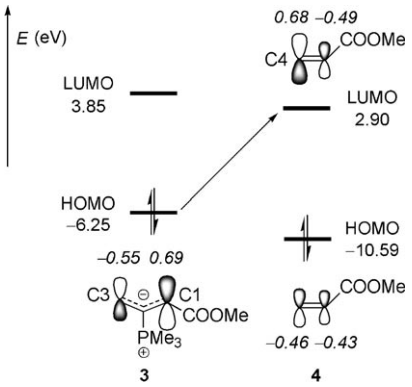

Figure 8. FMO diagram of the reaction between **3** and **4**. Orbital coefficients are given in italics.[25]

shows that α-**TS2** is lower in enthalpy and Gibbs free energy in benzene than γ-**TS2** by 1.5 and 1.2 kcal mol^{-1}, respectively.

Water-catalyzed [1,2]-proton shift: The formation of the cycloadduct α**-6** from reactants **1** and **4** and catalyst **2** is endergonic by about 11 kcal mol^{-1} in terms of free energy in benzene, which suggests that this transformation is not thermodynamically favorable. Therefore, the stepwise [3+2] cyclo-

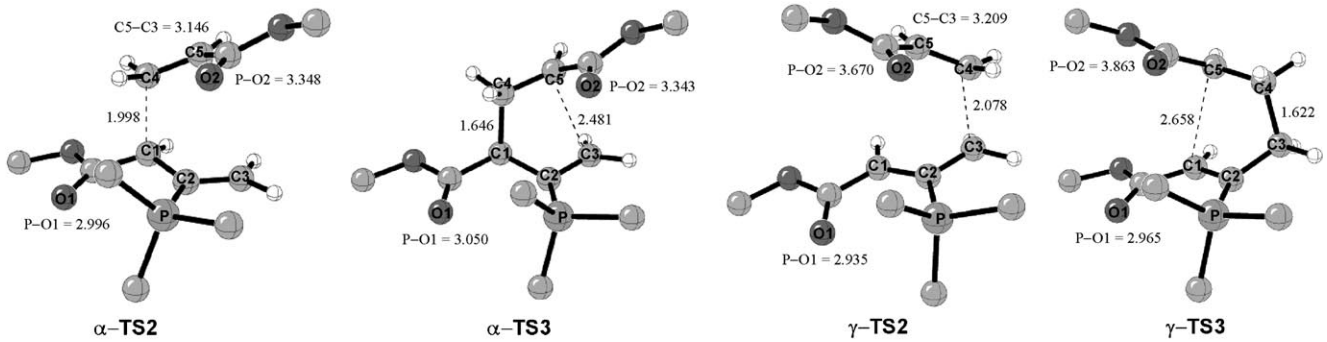

Figure 7. DFT-optimized structures of the transition states in the [3+2] cycloaddition of **3** and **4**. Distances are in Å. For clarity, each methyl group is represented by a carbon atom.

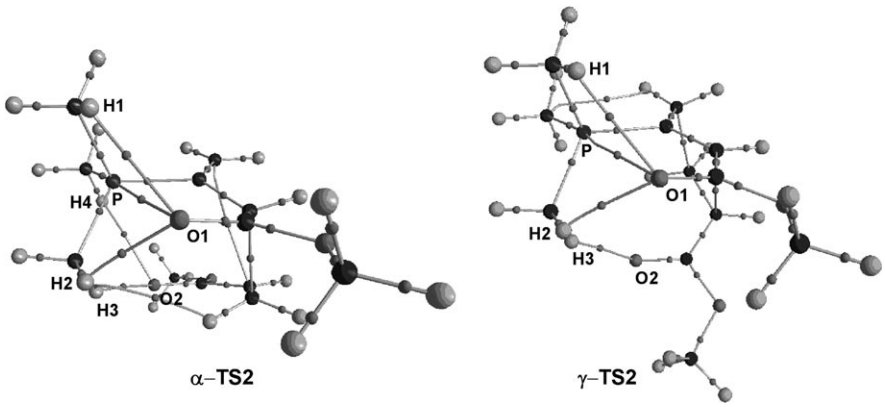

Figure 9. The bond critical points in the transition states α-**TS2** and γ-**TS2**.

Table 2. Electron density topological properties of selected (3,−1) critical points in the transition states α-**TS2** and γ-**TS2**.

Interaction	Distance [Å]	ρ	$\nabla^2\rho$	λ_1	λ_2	λ_3
P···O1 (α-**TS2**)	2.996	0.0129	0.0374	−0.0068	−0.0051	0.0493
H1···O1 (α-**TS2**)	2.361	0.0129	0.0461	−0.0130	−0.0093	0.0684
H2···O1 (α-**TS2**)	2.287	0.0151	0.0538	−0.0157	−0.0117	0.0812
H3···O2 (α-**TS2**)	2.204	0.0164	0.0556	−0.0178	−0.0163	0.0897
H4···O2 (α-**TS2**)	2.507	0.0092	0.0322	−0.0088	−0.0070	0.0480
P···O1 (γ-**TS2**)	2.935	0.0145	0.0398	−0.0085	−0.0062	0.0545
H1···O1 (γ-**TS2**)	2.365	0.0131	0.0470	−0.0133	−0.0089	0.0692
H2···O1 (γ-**TS2**)	2.237	0.0165	0.0605	−0.0175	−0.0127	0.0907
H3···O2 (γ-**TS2**)	2.127	0.0179	0.0622	−0.0205	−0.0190	0.1017

addition must be followed by an exergonic process to drive the whole reaction to completion. Calculations show that the subsequent [1,2]-proton transfer (conversion of **B** into **C**, Scheme 2) is exergonic by about 8 kcal mol^{-1}, which implies that the formation of **C** can drive the above stepwise [3+2] cycloaddition. This step can further drive the reaction to completion by generating the product and the catalyst. DFT calculations indicate that the activation free energy of a direct [1,2]-proton shift from α-**6** to **18** via **TS4** is 39.6 and 39.3 kcal mol^{-1} in benzene and in the gas phase, respectively (Figures 10 and 11). Because the phosphine-catalyzed [3+2] cycloaddition reaction is usually conducted at room temperature, this direct intramolecular [1,2]-proton shift pathway, requiring such a high activation free energy, is impossible from the viewpoint of kinetics.

The high activation energy for the [1,2]-proton shift can be easily understood in terms of orbital interactions[32] (Scheme 3). It is well known that the [1,2]-hydride shift for the carbocation is very facile with activation barriers of about 5 kcal mol^{-1}.[33] This process is a two-electron process and its transition state has a two-electron–two-orbital stabilizing interaction between the proton and the π orbital of the alkene. In contrast, the [1,2]-proton shift for the carbanion is a four-electron process and is difficult as the corresponding transition state involves a four-electron–two-orbital destabilizing interaction between the hydride and the π orbital of the alkene. The B3LYP/6-31+G(d)-computed activation free energy for the [1,2]-proton shift in the ethyl anion is 47.3 kcal mol^{-1} (Scheme 3, R=H).[34] In the phosphine-catalyzed [3+2] cycloaddition reaction, intermediate α-**6** is a zwitterionic species and its C2 atom (the atom numbering is given in Figure 11) is carbanionic, that is, it has more negative charge than the other carbon atoms. Thus, a [1,2]-hydrogen shift in α-**6** can be regarded as a [1,2]-proton shift of a carbanion and, consequently, a high activation energy is required for this intramolecular four-electron process.[35]

To obtain more information about the [1,2]-proton shift process in the [3+2] cycloaddition reaction, we conducted a PPh_3-catalyzed [3+2] cycloaddition of deuterium-labeled 2,3-butadienoate **7** (2-D incorporation level is about 95%) and fumarate **8** (reaction I, Scheme 4) in benzene (refluxed with sodium and freshly distilled prior to use). The 4-D- and 4-H-substituted products **9** and **10** were both obtained in a ratio of 75:25. This indicates that the [1,2]-proton transfer from α-**6** to **18** is not an intramolecular process.[36] If the [1,2]-hydrogen shift were a simple intramolecular process, the ratio of the 4-D- and 4-H-substituted products **9** and **10** would be about 95:5, in accord with the 2-D incorporation level of the allenoate **7**. Where does the extra 4-H-substituted product **10** come from? We speculated that the formation of extra

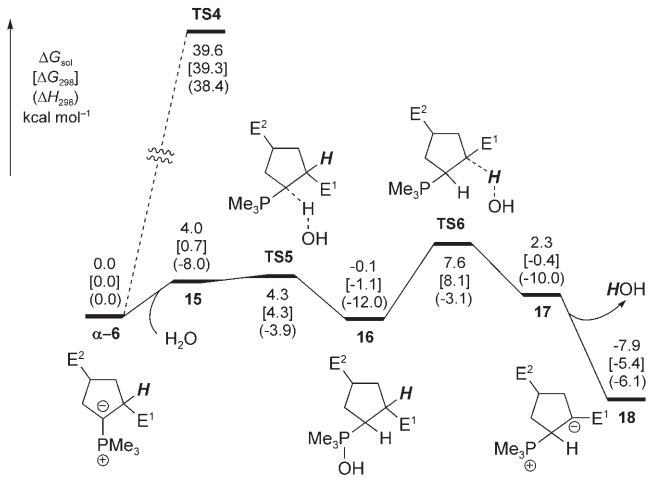

Figure 10. DFT-computed energy surface for the [1,2]-proton shift (E^1=E^2=CO_2Me).

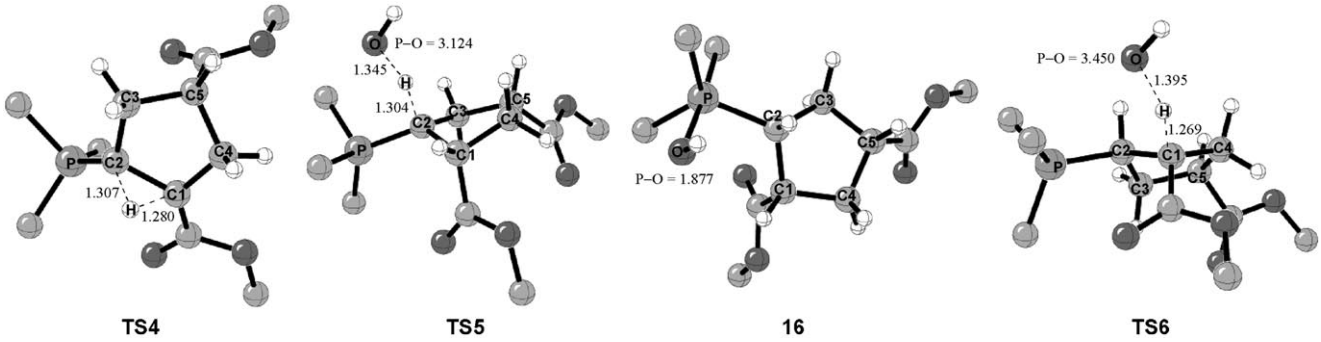

Figure 11. DFT-optimized structures of the transition states and intermediate **16** in the [1,2]-proton shift. Distances are in Å. For clarity, each methyl group is represented by a carbon atom.

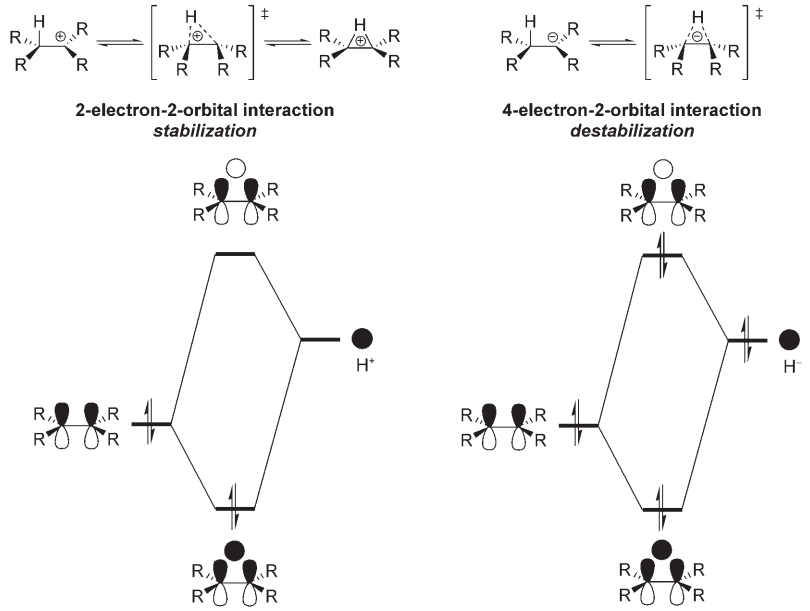

Scheme 3. Orbital interaction diagrams for the concerted [1,2]-hydrogen shifts in the carbanion and carbocation.

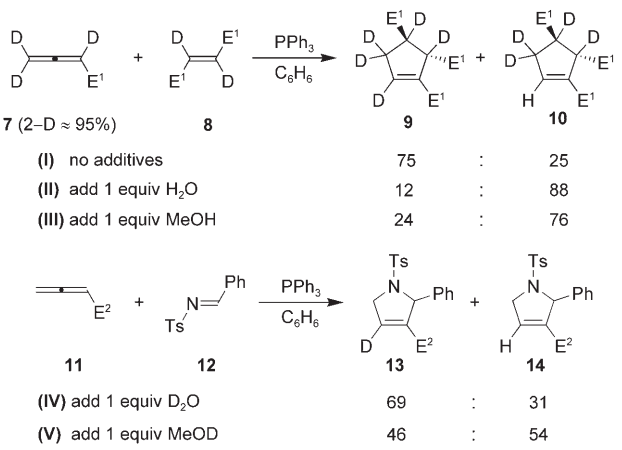

Scheme 4. Isotopic labeling experiments ($E^1 = CO_2Me$, $E^2 = CO_2Et$).

10 was due to the presence of a trace amount of water in the reaction system. To prove our hypothesis, we added 1 equiv. of H_2O to the [3+2] cycloaddition reaction between **7** and **8** (reaction II, Scheme 4). As expected, the ratio of the 4-H-substituted product **10** increased remarkably from 25 to 88%.[37,38] In a previous communication, we reported that control experiments showed that deuterium and hydrogen exchange occurred neither between water and the allenoate **7** nor between water and the [3+2] product **9**.[14] This has been further rationalized by DFT calculations which show that deuterium and hydrogen exchange between water and allenoate is disfavored compared with the [3+2] cycloaddition reaction. Discussions relating to this are presented in the Supporting Information. Besides, a further experiment indicated that water also catalyzes the [1,2]-proton shift in the phosphine-catalyzed hetero-[3+2] cycloaddition reaction between the allenoate and an electron-deficient imine (reaction IV, Scheme 4).

Computational studies were also conducted to reveal how a trace amount of water catalyzes the [1,2]-proton shift. The computed energy surface is depicted in Figure 10 and the optimized geometries of the transition states and one key intermediate **16** are shown in Figure 11. In the water-catalyzed [1,2]-proton shift process, α-**6** first reacts with water to form complex **15** with a reaction enthalpy of $-8.0\ kcal\,mol^{-1}$ and a reaction free energy of $4.0\ kcal\,mol^{-1}$ in benzene. Proton transfer from water to C2 (the atom numbering is given in Figure 11) via **TS5** requires only $0.3\ kcal\,mol^{-1}$ of activation free energy in benzene. A hydroxide anion is generated from water after donating a proton. Calculations indicate

that the generated hydroxide is not free in the reaction system. Instead, it forms a P–O bond with the phosphorus atom, as demonstrated by the P–O distance of 1.877 Å and the bond order of 0.43. The phosphorus-bound hydroxy group then acts as a base to deprotonate the hydrogen atom at C1. The deprotonation step to generate intermediate **17** via **TS6** is also facile and has an activation free energy of 7.7 kcal mol^{-1} in benzene. Dissociation of water from **17** leads to the formation of **18** which is exergonic by about 10 kcal mol^{-1} in terms of free energy in benzene.

The last step in the phosphine-catalyzed [3+2] cycloaddition reaction is to transform intermediate **18** into the final [3+2] product and to regenerate the phosphine catalyst (Figure 12). This process requires only 0.9 kcal mol^{-1} activation free energy and is exergonic by 33 kcal mol^{-1}.

Through the joint forces of computation and experiment, the catalytic role of a trace amount of water in the [1,2]-proton shift process has been discovered.[39–42] Further studies show that other protic sources, such as methanol, can catalyze the [1,2]-proton shift as well (reactions III and V, Scheme 4). Details of these experiments and calculations are given in the Supporting Information. In addition, about 8% 5-H-substituted products **9** and **10** were obtained in reaction III (Scheme 4), whereas no 5-D-substituted products **13** and **14** were found in reaction V (Scheme 4). This indicates that deuterium and hydrogen exchange occurred to some extent between deuterium-labeled allenoate **7** and the added methanol when fumarate was employed as the trapper. Through further calculations and experiments, we attributed these experimental results to a competition between H/D exchange and [3+2] cycloaddition. The extent of this competition depends on the concentration of the additives in benzene solution and the trappers used in the [3+2] cycloaddition reactions. Details of the relevant experiments, calculations, and discussions are given in the Supporting Information.

Kinetic studies: The DFT-computed energy surface for the complete catalytic cycle of the phosphine-catalyzed cycloaddition of allenoate **1** and alkene **4** is summarized in Figure 12 and reveals that the rate-determining step of the reaction is the [3+2] cycloaddition step and the activation free energy of the whole reaction is about 28 kcal mol^{-1}. However, the phosphine-catalyzed [3+2] cycloaddition reaction is usually completed at room temperature in a few hours, which indicates that the actual activation free energy is lower than the DFT-computed one. The overestimation of the computed activation barrier here can be easily understood considering that the [3+2] cycloaddition reaction is a multimolecular process and the computed ΔG_{sol} values are somewhat overestimated (owing to the overestimation of the entropic contributions in solution for a bi- or trimolecular process).[43] To obtain a more quantitative description of the mechanism, kinetic studies of the above [3+2] cycloaddition reaction are demanded. Such a study will also serve to test whether the DFT method used here is suitable or not for the study of this and other phosphine-catalyzed organocatalytic reactions. The information obtained from kinetic studies, such as rate constants and activation parameters, will greatly benefit the understanding of other related reactions and the design of novel phosphine-catalyzed reactions.

According to the computational results of the phosphine-catalyzed [3+2] cycloaddition reaction (Figure 12), the formation of the 1,3-dipole and the stepwise cycloaddition are difficult steps in the catalytic cycle. Therefore, in the simplified kinetic model for the [3+2] cycloaddition reaction (Scheme 5, k_1, k_{-1}, k_α, and k_γ are the corresponding rate constants), we assume that the formation of the 1,3-dipole is

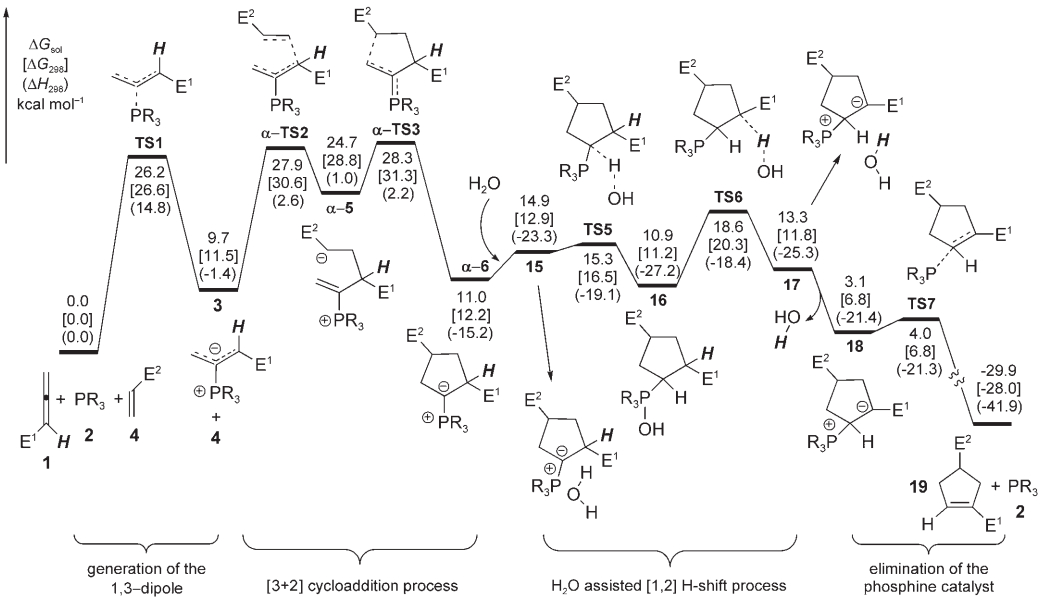

Figure 12. DFT-computed energy surface for the phosphine-catalyzed [3+2] cycloaddition reaction between **1** and **4** ($E^1 = E^2 = CO_2Me$, R = Me).

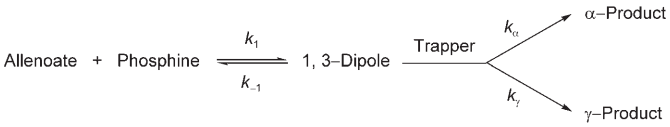

Scheme 5. The simplified kinetic model for phosphine-catalyzed [3+2] cycloaddition reaction.

reversible, but that the cycloaddition of the 1,3-dipole to the trapper by the α- or γ-addition mode is irreversible. These two assumptions are reasonable and consistent with the computed results shown in Figure 12. Based on our proposed kinetic model (Scheme 5), the rate constants and other kinetic parameters can be measured by kinetic studies [Eqs. (1)–(4)].

$$\frac{[\alpha\text{-product}]}{[\gamma\text{-product}]} = \frac{k_\alpha}{k_\gamma} \tag{1}$$

$$v_{\text{initial}} = \frac{\mathrm{d}[\alpha\text{-product}]}{\mathrm{d}t} = \frac{k_\alpha k_1[\text{allenoate}][\text{phosphine}][\text{trapper}]}{k_{-1} + (k_\alpha + k_\gamma)[\text{trapper}]} \tag{2}$$

$$\frac{[\text{allenoate}][\text{phosphine}]}{v_{\text{initial}}} = \frac{k_{-1}}{k_\alpha k_1}\frac{1}{[\text{trapper}]} + \frac{k_\alpha + k_\gamma}{k_\alpha k_1} \tag{3}$$

$$Y = \frac{k_{-1}}{k_\alpha k_1}X + \frac{k_\alpha + k_\gamma}{k_\alpha k_1} \tag{4}$$

The kinetic studies were conducted for the reaction between ethyl allenoate and methyl acrylate in the presence of triphenylphosphine as catalyst. From the kinetic model [the detailed derivation of Equations (1) and (2) and the experimental details are given in the Supporting Information], the ratio of k_α/k_γ is equal to the ratio of the [3+2] cycloadducts generated from the two cycloaddition pathways [Eq. (1)]. This ratio can be measured by gas phase chromatography (GC), which can also be used to determine the initial reaction rate [the rate of α-product formation, Eq. (2)] at a low conversion of allenoate. Equation (2) can be rearranged to Equation (3) to give an important linear relationship. The value of the [allenoate][phosphine]/v_{initial} ratio [denoted as Y in Eq. (4)] only depends on the reciprocal of the trapper's concentration [1/[trapper], denoted as X in Eq. (4)] at a given temperature. Thus, a series of values for the [allenoate][phosphine]/v_{initial} ratio were determined at different concentrations of the trapper at the same temperature. Through a simple linear regression, both intercept and slope can be obtained. Based on the values of the k_α/k_γ ratio and intercept, the rate constant for the formation of the 1,3-dipole (k_1) can be calculated. Then the value of the k_α/k_{-1} or k_γ/k_{-1} ratio can be obtained according to the slope. We conducted our kinetic studies at four different temperatures (Figure 13) and derived the activation parameters from the Eyring equation for the first two steps of the phosphine-catalyzed [3+2] cycloaddition reaction, the generation of the 1,3-dipole and its subsequent cycloaddition to the dipolarophile (for details, see the Supporting Information). The kinetic results are summarized in Table 3.

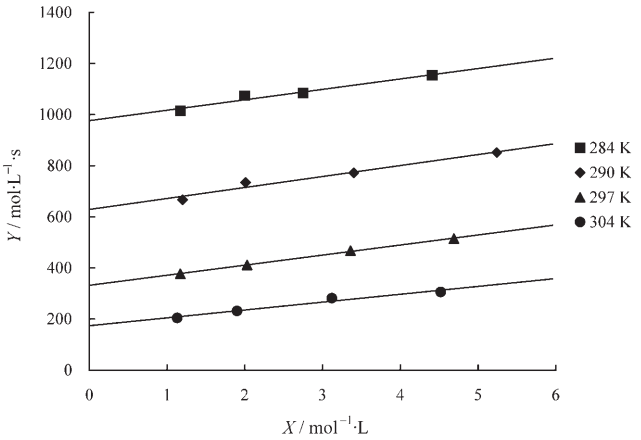

Figure 13. The relationship between X and Y at different temperatures.

The experimentally measured activation free energies, enthalpies, and entropies are summarized in Figure 14 and Table 4. For comparison, the DFT-computed values are also given in Table 4. The data show that the rate-determining step of the phosphine-catalyzed [3+2] cycloaddition reaction of allenoate **1** and alkene **4** is the generation of the 1,3-dipole with a measured activation free energy of 20.6 kcal mol^{-1} in benzene. The transition states of the [3+2] cycloaddition processes from the α- and γ-position (19.6 and 20.1 kcal mol^{-1}, with respect to the reactants) have Gibbs free energies very close to that of the transition state **TS-1**. These data indicate that the formation of the 1,3-dipole is more difficult than the stepwise [3+2] cycloaddition process. However, the [3+2] cycloaddition step might also become rate-determining if the phosphine catalyst or the trapper is changed. No matter which step is rate-determining, it is evident that the first two steps of the [3+2] cycloaddition reaction, the generation of the 1,3-dipole and its subsequent cycloaddition to a dipolarophile, are crucial to understand the whole reaction process. Besides, the experimentally determined activation enthalpies for both the 1,3-dipole formation and the [3+2] cycloaddition are quite close to the DFT-computed ones (Table 4). The computed activation entropies are higher than the experimental ones (Table 4), further confirming the overestimation of entropy in computing bi- or trimolecular processes. The overestimated activation free energies in solution are indeed a result of the overestimation of the entropic contributions in solu-

Table 3. Experimentally measured values of k_α/k_γ, k_1, k_α/k_{-1}, and k_γ/k_{-1} at different temperatures.

T [K]	k_α/k_γ	k_1 [10^{-3} L mol^{-1} s^{-1}]	k_α/k_{-1}	k_γ/k_{-1}
284	3.09	1.36±0.02	18.0±2.6	5.83±0.83
290	2.88	2.14±0.06	10.9±1.4	3.78±0.48
297	2.56	4.19±0.04	6.06±0.15	2.37±0.06
304	2.52	8.03±0.55	4.06±0.53	1.61±0.21

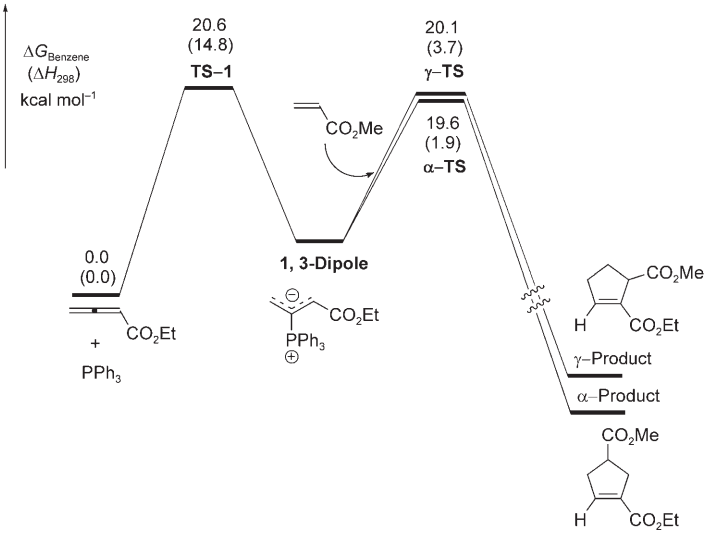

Figure 14. Experimentally measured activation free energies and enthalpies for the 1,3-dipole generation and the [3+2] cycloaddition.

Table 4. Activation parameters determined from calculations and experiments.

	TS-1	α-TS	γ-TS
ΔH computed in the gas phase [kcal mol^{-1}]	14.8	2.2	4.0
ΔH measured in benzene [kcal mol^{-1}]	14.8 ± 0.7	1.9 ± 0.6	3.7 ± 0.3
ΔS computed in the gas phase [cal K^{-1} mol^{-1}]	−39.6	−97.7	−91.3
ΔS measured in benzene [cal K^{-1} mol^{-1}]	−19.6 ± 1.7	−59.6 ± 2.2	−55.2 ± 1.0

tion.[23,43] The computed entropic contribution in the gas phase should be taken as an upper limit in solution; the actual value in such systems is 50–60 % of the computed gas phase value.

Alkynoate as the precursor of the 1,3-dipole and a water-catalyzed [1,3]-hydrogen shift: In addition to the method of in situ generation of the 1,3-dipole from allenoate and phosphine, alkynoates can also be used as an alternative three-carbon synthon to give the 1,3-dipole when phosphine is used as a catalyst. This provides another important approach to nucleophilic phosphine catalysis. In our model reaction we computed this process by using methyl 2-butynoate (**20**) and trimethylphosphine (**2**) as the starting materials. The computed energy surface is given in Figure 15, and the optimized geometries are shown in Figure 16.

As shown in Figure 15, the nucleophilic attack of phosphine **2** on alkynoate **20** requires an activation free energy of 29.2 kcal mol^{-1} in benzene and an activation enthalpy of 17.6 kcal mol^{-1}.[44] In addition, the geometry optimization of **TS8** shows that the length of the forming P–C2 bond is 2.147 Å (the atom numbering is given in Figure 16). However, the formation of the 1,3-dipole **21** is a highly endergonic process (by 23.2 kcal mol^{-1} in terms of free energy and 14.2 kcal mol^{-1} in terms of enthalpy). Consequently, the formation of **21** must be followed by an exergonic process to drive this reaction forward. Conversion of **21** into **3** is the process of choice, which is exergonic by 16.3 kcal mol^{-1} in free energy and 19.7 kcal mol^{-1} in enthalpy. At this stage, it is necessary to discuss the mechanistic details of the conversion of **21** into **3**.

The most obvious pathway connecting these two 1,3-dipoles is a concerted [1,3]-proton shift process. Geometry optimization of **TS9** shows that the lengths of the forming and breaking C–H bonds are 1.414 and 1.541 Å, respectively. Unfortunately, this concerted step is extremely energy-demanding with an activation free energy of 52.8 kcal mol^{-1} in benzene and an activation enthalpy of 51.1 kcal mol^{-1}. As a result, this concerted [1,3]-proton shift cannot be achieved under mild reaction conditions (usually room temperature is used for phosphine-catalyzed [3+2] cycloaddition reactions with alkynoates as the three-carbon synthon). In view of the mechanism of the [3+2] cycloaddition reaction discussed above, we proposed that a trace amount of water present in the so-called "anhydrous" reaction mixture could also play a catalytic role in the [1,3]-proton shift process.[45]

Computational results show that the water-catalyzed [1,3]-proton transfer is very facile. First, a water–dipole complex **22** is formed between **21** and water with a reaction enthalpy of −7.4 kcal mol^{-1} and a reaction free energy of 3.6 kcal mol^{-1} in benzene. Then the olefinic anion moiety of **21** is quickly protonated by water via **TS10** with a very low energy barrier.[46] Conversion of **22** into **23** is exergonic by 12.6 kcal mol^{-1} in terms of free energy. In intermediate **23** the in situ generated hydroxide anion is coordinated to the

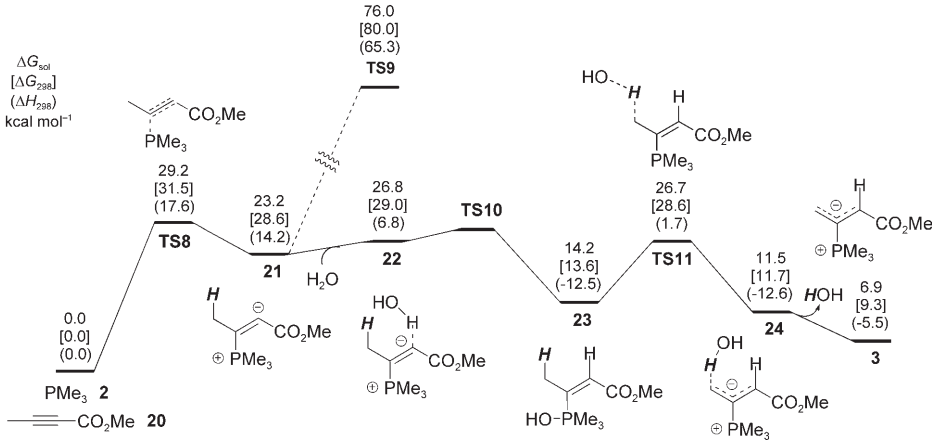

Figure 15. DFT-computed energy surface for the formation of the 1,3-dipole **3** from PMe_3 and alkynoate.

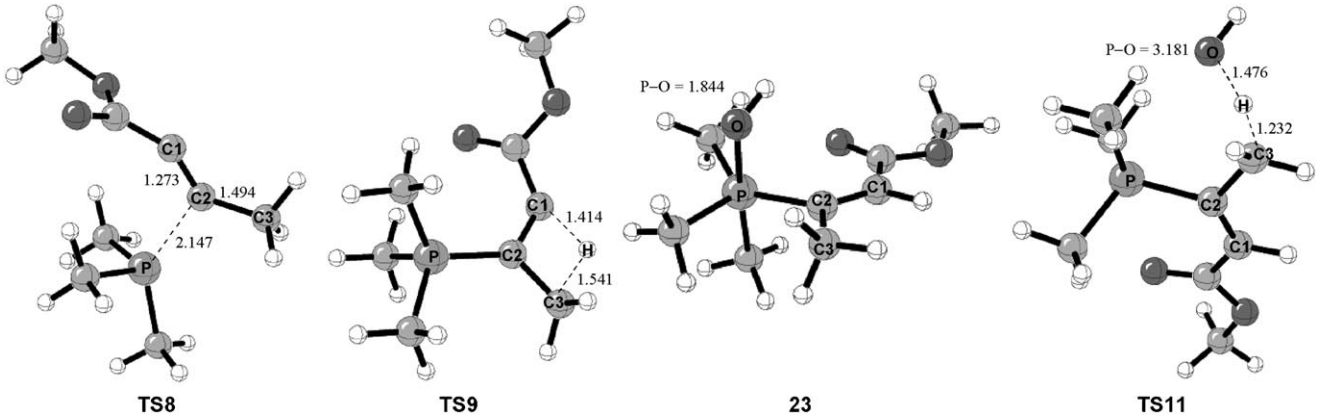

Figure 16. DFT-optimized geometries of the transition states and intermediate **23** in the formation of the 1,3-dipole **3** from PMe_3 and alkynoate. Distances are in Å.

phosphorus atom. From **23**, deprotonation of the γ-hydrogen atom is very facile, requiring an activation free energy of 12.5 kcal mol^{-1}. Geometry optimization of **TS11** shows that the O–H and H–C3 distances are 1.476 and 1.232 Å, respectively. Once this energy barrier to deprotonation has been overcome, the reaction process goes downhill to give the 1,3-dipole **3**. An isotopic labeling experiment (Scheme 6)

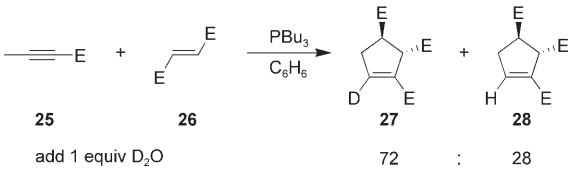

Scheme 6. Isotopic labeling experiment (E = CO_2Et).

also supported the involvement of water in the [3+2] cycloaddition reaction involving alkynoate.[47] Further computational studies indicate that other protic sources (e.g., methanol) can catalyze such a [1,3]-proton shift as well (see the Supporting Information). These results also explain why the phosphine-catalyzed isomerization of alkynoates to the corresponding dienoates works better in the presence of some protic sources such as acetic acid or ethanol.[48]

Conclusion

The detailed mechanism of Lu's phosphine-catalyzed [3+2] cycloaddition reaction between allenoates and electron-deficient alkenes has been investigated. The generation of a 1,3-dipole is the first step of the phosphine-catalyzed [3+2] cycloaddition reaction and is also key to all nucleophilic phosphine-catalyzed reactions. Through computational studies (DFT calculations and FMO analysis), the thermodynamics and kinetics relating to the formation of the 1,3-dipole have been obtained and suggest that electron-withdrawing groups in allenes can stabilize both the transition state and the 1,3-dipole. The relationship between all the possible structures of the 1,3-dipoles and their energies has been analyzed and the results indicate that the interaction between the phosphorus and carbonyl oxygen atoms is very important for the stabilization.

The stepwise [3+2] cycloaddition between the in situ generated 1,3-dipole and an unsymmetrical alkene can lead to regioisomeric cycloadducts. This regioselectivity can be easily rationalized by FMO theory and AIM analysis. Hydrogen bonding in the stepwise [3+2] process is also critical to the relative stabilities of the α- and γ-addition transition states.

Another important and interesting phenomenon in the [3+2] cycloaddition reaction is the [1,2]- or [1,3]-hydrogen shift (when the 1,3-dipole is generated from alkynoate and phosphine). Calculations indicate that the commonly accepted intramolecular [1,2]- and [1,3]-hydrogen shifts are impossible owing to very high activation barriers. Further isotopic labeling experiments and computations corroborate with each other and demonstrate that water or other protic sources can catalyze [1,2]- and [1,3]-proton shifts with very low activation free energies. The discovery of the catalytic role of a trace amount of water in phosphine-catalyzed [3+2] cycloaddition reactions will help chemists understand some other "anhydrous" reactions in which a [1,*n*]-hydrogen shift is implicated.

Kinetic studies of the phosphine-catalyzed [3+2] cycloaddition reaction suggest that formation of the 1,3-dipole from allenoate and phosphine and its stepwise [3+2] cycloaddition to an electron-deficient alkene are energy-demanding processes with Gibbs free energies of about 20 kcal mol^{-1} in benzene solution.

The information obtained from the mechanistic studies of phosphine-catalyzed [3+2] cycloaddition reactions, both computationally and experimentally, will greatly deepen our understanding of other related phosphine-catalyzed reactions and assist the design of novel phosphine-catalyzed reactions. The discovery that a trace amount of water acts as a catalyst in [1,2]- and [1,3]-proton shifts will prompt chemists to rethink the role of water and other protic sources in organic reactions.[49]

Acknowledgements

We are indebted to generous financial support from a new faculty grant from the 985 Program for Excellent Research in Peking University, the Natural Science Foundation of China (20772007 and 20672005), and the Scientific Research Foundation for Returned Overseas Chinese Scholars, State Education Ministry of China.

[1] R. Huisgen, *Angew. Chem.* **1963**, *75*, 604; *Angew. Chem. Int. Ed. Engl.* **1963**, *2*, 565.

[2] For reviews, see: a) A. Padwa, M. D. Weingarten, *Chem. Rev.* **1996**, *96*, 223; b) K. V. Gothelf, K. A. Jorgensen, *Chem. Rev.* **1998**, *98*, 863; c) G. Mehta, S. Muthusamy, *Tetrahedron* **2002**, *58*, 9477; d) C. Najera, J. M. Sansano, *Curr. Org. Chem.* **2003**, *7*, 1105; e) I. Coldham, R. Hufton, *Chem. Rev.* **2005**, *105*, 2765; f) G. Pandey, P. Banerjee, S. R. Gadre, *Chem. Rev.* **2006**, *106*, 4484; g) D. H. Ess, G. O. Jones, K. N. Houk, *Adv. Synth. Catal.* **2006**, *348*, 2337.

[3] a) R. L. Danheiser, D. J. Carini, A. Basak, *J. Am. Chem. Soc.* **1981**, *103*, 1604; b) R. L. Danheiser, C. A. Kwasigroch, Y. M. Tsai, *J. Am. Chem. Soc.* **1985**, *107*, 7233.

[4] a) B. M. Trost, D. M. T. Chan, *J. Am. Chem. Soc.* **1983**, *105*, 2315; b) B. M. Trost, D. M. T. Chan, *J. Am. Chem. Soc.* **1983**, *105*, 2326; c) B. M. Trost, *Angew. Chem.* **1986**, *98*, 1; *Angew. Chem. Int. Ed. Engl.* **1986**, *25*, 1.

[5] a) C. Zhang, X. Lu, *J. Org. Chem.* **1995**, *60*, 2906; b) Z. Xu, X. Lu, *Tetrahedron Lett.* **1997**, *38*, 3461; c) Z. Xu, X. Lu, *J. Org. Chem.* **1998**, *63*, 5031; d) Z. Xu, X. Lu, *Tetrahedron Lett.* **1999**, *40*, 549.

[6] For selected very recent reports about [3+2] cycloaddition reactions, see: a) A. K. Sahoo, S. Mori, H. Shinokubo, A. Osuka, *Angew. Chem.* **2006**, *118*, 8140; *Angew. Chem. Int. Ed.* **2006**, *45*, 7972; b) M. Gulias, R. Garcia, A. Delgado, L. Castedo, J. L. Mascarenas, *J. Am. Chem. Soc.* **2006**, *128*, 384; c) J. Barluenga, R. Vicente, L. A. Lopez, M. Tomas, *J. Am. Chem. Soc.* **2006**, *128*, 7050; d) J.-J. Lian, P.-C. Chen, Y.-P. Liu, H.-C. Ting, R.-S. Liu, *J. Am. Chem. Soc.* **2006**, *128*, 11372; e) P. Restorp, A. Fischer, P. Somfai, *J. Am. Chem. Soc.* **2006**, *128*, 12646; f) A. Herath, J. Montgomery, *J. Am. Chem. Soc.* **2006**, *128*, 14030; g) H.-T. Chang, T. T. Jayanth, C.-H. Cheng, *J. Am. Chem. Soc.* **2007**, *129*, 4166; h) X. Huang, L. Zhang, *J. Am. Chem. Soc.* **2007**, *129*, 6398; i) S. Diez-Gonzalez, A. Correa, L. Cavallo, S. P. Nolan, *Chem. Eur. J.* **2006**, *12*, 7558; j) Y. Cheng, M.-F. Liu, D.-C. Fang, X.-M. Lei, *Chem. Eur. J.* **2007**, *13*, 4282.

[7] For a recent thematic issue on organocatalysis, see: K. N. Houk, B. List, *Acc. Chem. Res.* **2004**, *37*, 487, and references therein.

[8] a) Y. Du, X. Lu, *J. Org. Chem.* **2003**, *68*, 6463; b) J.-C. Wang, M. J. Krische, *Angew. Chem.* **2003**, *115*, 6035; *Angew. Chem. Int. Ed.* **2003**, *42*, 5855; c) T. Q. Pham, S. G. Pyne, B. W. Skelton, A. H. White, *J. Org. Chem.* **2005**, *70*, 6369.

[9] a) G. Zhu, Z. Chen, Q. Jiang, D. Xiao, P. Cao, X. Zhang, *J. Am. Chem. Soc.* **1997**, *119*, 3836; b) J. E. Wilson, G. C. Fu, *Angew. Chem.* **2006**, *118*, 1454; *Angew. Chem. Int. Ed.* **2006**, *45*, 1426; c) B. J. Cowen, S. J. Miller, *J. Am. Chem. Soc.* **2007**, *129*, 10988.

[10] For selected recent examples, see: a) L.-C. Wang, A. L. Luis, K. Agapiou, H.-Y. Jang, M. J. Krische, *J. Am. Chem. Soc.* **2002**, *124*, 2402; b) S. A. Frank, D. J. Mergott, W. R. Roush, *J. Am. Chem. Soc.* **2002**, *124*, 2404; c) A. T. Ung, K. Schafer, K. B. Lindsay, S. G. Pyne, K. Amornraksa, R. Wouters, I. van der Linden, I. Biesmans, A. S. J. Lesage, B. W. Skelton, A. H. White, *J. Org. Chem.* **2002**, *67*, 227; d) B. Liu, R. Davis, B. Joshi, D. W. Reynolds, *J. Org. Chem.* **2002**, *67*, 4595; e) Y. Du, X. Lu, Y. Yu, *J. Org. Chem.* **2002**, *67*, 8901; f) C. Lu, X. Lu, *Org. Lett.* **2002**, *4*, 4677; g) J.-C. Wang, S.-S. Ng, M. J. Krische, *J. Am. Chem. Soc.* **2003**, *125*, 3682; h) X.-F. Zhu, J. Lan, O. Kwon, *J. Am. Chem. Soc.* **2003**, *125*, 4716; i) C. A. Evans, S. J. Miller, *J. Am. Chem. Soc.* **2003**, *125*, 12394; j) H. Kuroda, I. Tomita, T. Endo, *Org. Lett.* **2003**, *5*, 129; k) C.-K. Jung, J.-C. Wang, M. J. Krische, *J. Am. Chem. Soc.* **2004**, *126*, 4118; l) R.-H. Fan, X.-L. Hou, L.-X. Dai, *J. Org. Chem.* **2004**, *69*, 689; m) S. Kamijo, C. Kanazawa, Y. Yamamoto, *J. Am. Chem. Soc.* **2005**, *127*, 9260; n) R. P. Wurz, G. C. Fu, *J. Am. Chem. Soc.* **2005**, *127*, 12234; o) X.-F. Zhu, C. E. Henry, J. Wang, T. Dudding, O. Kwon, *Org. Lett.* **2005**, *7*, 1387; p) Y. Du, J. Feng, X. Lu, *Org. Lett.* **2005**, *7*, 1987; q) X.-F. Zhu, A.-P. Schaffner, R. C. Li, O. Kwon, *Org. Lett.* **2005**, *7*, 2977; r) Y. S. Tran, O. Kwon, *Org. Lett.* **2005**, *7*, 4289; s) V. Nair, A. T. Biju, K. Mohanan, E. Suresh, *Org. Lett.* **2006**, *8*, 2213; t) S. Castellano, H. D. G. Fiji, S. S. Kinderman, M. Watanabe, P. de Leon, F. Tamanoi, O. Kwon, *J. Am. Chem. Soc.* **2007**, *129*, 5843; u) D. J. Wallace, R. L. Sidda, R. A. Reamer, *J. Org. Chem.* **2007**, *72*, 1051; v) C. E. Henry, O. Kwon, *Org. Lett.* **2007**, *9*, 3069; w) L.-W. Ye, X.-L. Sun, Q.-G. Wang, Y. Tang, *Angew. Chem.* **2007**, *119*, 6055; *Angew. Chem. Int. Ed.* **2007**, *46*, 5951.

[11] For reviews on phosphine-catalyzed reactions, see: a) X. Lu, C. Zhang, Z. Xu, *Acc. Chem. Res.* **2001**, *34*, 535; b) J. L. Methot, W. R. Roush, *Adv. Synth. Catal.* **2004**, *346*, 1035; c) X. Lu, Y. Du, C. Lu, *Pure Appl. Chem.* **2005**, *77*, 1985.

[12] For selected reviews on allene chemistry, see: a) R. Zimmer, C. U. Dinesh, E. Nandanan, F. A. Khan, *Chem. Rev.* **2000**, *100*, 3067; b) L. K. Sydnes, *Chem. Rev.* **2003**, *103*, 1133; c) S. Ma, *Chem. Rev.* **2005**, *105*, 2829.

[13] a) T. Q. Pham, S. G. Pyne, B. W. Skelton, A. H. White, *Tetrahedron Lett.* **2002**, *43*, 5953; b) T. Dudding, O. Kwon, E. Mercier, *Org. Lett.* **2006**, *8*, 3643; after we published our preliminary results describing the discovery of the water-catalyzed [1,2]-hydrogen shift by computation and experiment (see ref. [14]), Dudding, Kwon and co-workers later reached the same conclusion through DFT calculations, see: c) E. Mercier, B. Fonovic, C. Henry, O. Kwon, T. Dudding, *Tetrahedron Lett.* **2007**, *48*, 3617.

[14] Y. Xia, Y. Liang, Y. Chen, M. Wang, L. Jiao, F. Huang, S. Liu, Y. Li, Z.-X. Yu, *J. Am. Chem. Soc.* **2007**, *129*, 3470.

[15] Gaussian 03 (Revision C.02), M. J. Frisch, G. W. Trucks, H. B. Schlegel, G. E. Scuseria, M. A. Robb, J. R. Cheeseman, J. A. Montgomery, Jr., T. Vreven, K. N. Kudin, J. C. Burant, J. M. Millam, S. S. Iyengar, J. Tomasi, V. Barone, B. Mennucci, M. Cossi, G. Scalmani, N. Rega, G. A. Petersson, H. Nakatsuji, M. Hada, M. Ehara, K. Toyota, R. Fukuda, J. Hasegawa, M. Ishida, T. Nakajima, Y. Honda, O. Kitao, H. Nakai, M. Klene, X. Li, J. E. Knox, H. P. Hratchian, J. B. Cross, C. Adamo, J. Jaramillo, R. Gomperts, R. E. Stratmann, O. Yazyev, A. J. Austin, R. Cammi, C. Pomelli, J. W. Ochterski, P. Y. Ayala, K. Morokuma, G. A. Voth, P. Salvador, J. J. Dannenberg, V. G. Zakrzewski, S. Dapprich, A. D. Daniels, M. C. Strain, O. Farkas, D. K. Malick, A. D. Rabuck, K. Raghavachari, J. B. Foresman, J. V. Ortiz, Q. Cui, A. G. Baboul, S. Clifford, J. Cioslowski, B. B. Stefanov, G. Liu, A. Liashenko, P. Piskorz, I. Komaromi, R. L. Martin, D. J. Fox, T. Keith, M. A. Al-Laham, C. Y. Peng, A. Nanayakkara, M. Challacombe, P. M. W. Gill, B. Johnson, W. Chen, M. W. Wong, C. Gonzalez, J. A. Pople, Gaussian, Inc., Wallingford, CT, **2004**.

[16] a) A. D. Becke, *J. Chem. Phys.* **1993**, *98*, 5648; b) C. Lee, W. Yang, R. G. Parr, *Phys. Rev. B* **1988**, *37*, 785.

[17] W. J. Hehre, L. Radom, P. v. R. Schleyer, J. A. Pople, *Ab Initio Molecular Orbital Theory*, Wiley, New York, **1986**.

[18] a) M. J. Frisch, J. A. Pople, J. E. Del Bene, *J. Chem. Phys.* **1983**, *78*, 4063; b) J. E. Del Bene, H. D. Mettee, M. J. Frisch, B. T. Luke, J. A. Pople, *J. Phys. Chem.* **1983**, *87*, 3279; c) J. Gao, D. S. Garner, W. L. Jorgensen, *J. Am. Chem. Soc.* **1986**, *108*, 4784; d) Y.-D. Wu, D.-F. Wang, J. L. Sessler, *J. Org. Chem.* **2001**, *66*, 3739.

[19] a) K. Fukui, *J. Phys. Chem.* **1970**, *74*, 4161; b) C. Gonzalez, H. B. Schlegel, *J. Chem. Phys.* **1989**, *90*, 2154; c) C. Gonzalez, H. B. Schlegel, *J. Phys. Chem.* **1990**, *94*, 5523.

[20] a) V. Barone, M. Cossi, *J. Phys. Chem. A* **1998**, *102*, 1995; b) M. Cossi, N. Rega, G. Scalmani, V. Barone, *J. Comput. Chem.* **2003**, *24*, 669; c) Y. Takano, K. N. Houk, *J. Chem. Theory Comput.* **2005**, *1*, 70.

[21] a) K. B. Wiberg, *Tetrahedron* **1968**, *24*, 1083; b) A. E. Reed, L. A. Curtiss, F. Weinhold, *Chem. Rev.* **1988**, *88*, 899.

[22] R. F. W. Bader, *Atoms in Molecules: A Quantum Theory*, Clarendon Press, Oxford, **1990**.

[23] DFT calculations at the B3LYP/6-31+G(d)//B3LYP/3-21G level show that PMe_3 is more efficient than PPh_3 in generating the 1,3-

dipole. The activation energy of the former is lower than that of the latter by 3.2 kcal mol^{-1} (14.9 versus 18.1 kcal mol^{-1} in terms of electronic energy without ZPVE corrections). We have also tested the suitability of MP2 calculations in the present system. However, the activation energy for the generation of the 1,3-dipole using PMe_3 is 7.1 kcal mol^{-1} at the MP2//B3LYP/6-31+G(d) level, which is 7.3 kcal mol^{-1} lower than that computed at the B3LYP/6-31+G(d) level. Therefore, we concluded that the MP2 method was not appropriate for the study of the reaction system described herein.

[24] a) H. E. Zimmerman, *Acc. Chem. Res.* **1971**, *4*, 272; b) K. N. Houk, *Acc. Chem. Res.* **1975**, *8*, 361; c) I. Fleming, *Frontier Orbitals and Organic Chemical Reactions*, Wiley, New York, **1976**.

[25] The molecular orbital energies were computed at the HF/6-31G(d) level and the molecular orbital coefficients at the HF/STO-3G level, which were all based on the B3LYP/6-31+G(d) gas-phase geometries.

[26] X.-F. Zhu, C. E. Henry, O. Kwon, *J. Am. Chem. Soc.* **2007**, *129*, 6722.

[27] For a recent discussion on R_3N^+–C–H···O=C hydrogen bonding, see: C. E. Cannizzaro, K. N. Houk, *J. Am. Chem. Soc.* **2002**, *124*, 7163.

[28] U. Koch, P. L. A. Popelier, *J. Phys. Chem.* **1995**, *99*, 9747.

[29] There are four possible approaches for the addition of the 1,3-dipole **3** to methyl acrylate (**4**) based on their relative orientations (α-**TS2**, α-**TS2′**, γ-**TS2**, and γ-**TS2′**). Calculations indicate that α-**TS2′** and γ-**TS2′** are generally more unfavorable than α-**TS2** and γ-**TS2** by more than 4 kcal mol^{-1}. For details, see the Supporting Information.

[30] For a recent theoretical explanation of the relative reactivities of the 1,3-dipoles in Huisgen [3+2] cycloaddition reactions, see: D. H. Ess, K. N. Houk, *J. Am. Chem. Soc.* **2007**, *129*, 10646.

[31] The regiochemistry of this process was the focus of previous theoretical studies. Dudding et al. pointed out that there are three key factors determining the regioselectivity: 1) Lewis acid activation, 2) strong hydrogen bonding, and 3) the minimization of unfavorable van der Waals contacts. For details, see ref. [13b].

[32] R. B. Woodward, R. Hoffmann, *Angew. Chem.* **1969**, *81*, 797; *Angew. Chem. Int. Ed. Engl.* **1969**, *8*, 781.

[33] I. V. Vrèek, V. Vrèek, H.-U. Siehl, *J. Phys. Chem. A* **2002**, *106*, 1604.

[34] The MP2/6-31+G(d) computed activation free energy for the [1,2]-proton shift of the ethyl anion is 49.1 kcal mol^{-1}, which is similar to the result obtained by DFT calculations. A similar process involving a direct [1,2]-proton shift of an alkoxide to a hydroxy carbanion is also difficult, see: S. Gronert, *Org. Lett.* **2007**, *9*, 3065.

[35] The four-elctron intramolecular [1,2]-proton-shift transition state is Hückel anti-aromatic, see: E. V. Anslyn, D. A. Dougherty, *Modern Physical Organic Chemistry*, University Science Books, Sausalito, **2005**.

[36] Previous calculations demonstrated that the intermolecular hydrogen shift between two α-**6** molecules was unfavorable compared with the water-catalyzed process. For details, see the Supporting Information of ref. [14].

[37] We repeated the PPh_3-catalyzed [3+2] cycloaddition of deuterium-labeled reactants **7** and **8** which had been stored in the refrigerator for 14 months in benzene (refluxed with sodium and freshly distilled prior to use). It was found that the ratio of the 4-H-substituted product **10** had increased from the previous 25% to a new value of 52%. We attributed the increase in the percentage of **10** in the final products to an increase of moisture in **7** and **8** during storage. This indicates that the level of incorporation of protons in the final cycloadduct depends on their content (from H_2O) in the reaction system.

[38] One equivalent of H_2O can provide twice as many protons as MeOH. This suggests that 0.5 equivalents of H_2O is as effective as 1 equivalent of MeOH in providing the same number of protons for the water-catalyzed [1,2]-proton shift. This was supported by the comparison experiment: when 0.5 equivalents of H_2O was added to the [3+2] cycloaddition reaction between **7** and **8**, the ratio of the 4-D and 4-H substituted products **9** and **10** was 24:76. This ratio is coincidently the same as that of reaction III in Scheme 4, in which 1 equivalent of MeOH was added as the additive.

[39] For selected reviews on reactions involving water, see: a) R. Breslow, *Acc. Chem. Res.* **1991**, *24*, 159; b) S. Kobayashi, K. Manabe, *Acc. Chem. Res.* **2002**, *35*, 209; c) U. M. Lindstrom, *Chem. Rev.* **2002**, *102*, 2751; d) C.-J. Li, *Chem. Rev.* **2005**, *105*, 3095; e) M. C. Pirrung, *Chem. Eur. J.* **2006**, *12*, 1312; f) A. P. Brogan, T. J. Dickerson, K. D. Janda, *Angew. Chem.* **2006**, *118*, 8278; *Angew. Chem. Int. Ed.* **2006**, *45*, 8100; g) Y. Hayashi, *Angew. Chem.* **2006**, *118*, 8281; *Angew. Chem. Int. Ed.* **2006**, *45*, 8103; h) D. G. Blackmond, A. Armstrong, V. Coombe, A. Wells, *Angew. Chem.* **2007**, *119*, 3872; *Angew. Chem. Int. Ed.* **2007**, *46*, 3798.

[40] For selected very recent reports on reactions involving water, see: a) Y. Hayashi, T. Sumiya, J. Takahashi, H. Gotoh, T. Urushima, M. Shoji, *Angew. Chem.* **2006**, *118*, 972; *Angew. Chem. Int. Ed.* **2006**, *45*, 958; b) S. Tiwari, A. Kumar, *Angew. Chem.* **2006**, *118*, 4942; *Angew. Chem. Int. Ed.* **2006**, *45*, 4824; c) T. Kurahashi, H. Shinokubo, A. Osuka, *Angew. Chem.* **2006**, *118*, 6484; *Angew. Chem. Int. Ed.* **2006**, *45*, 6336; d) L. Zhang, S. Wang, *J. Am. Chem. Soc.* **2006**, *128*, 1442; e) M. Carril, R. SanMartin, I. Tellitu, E. Dominguez, *Org. Lett.* **2006**, *8*, 1467; f) X. Yao, C.-J. Li, *Org. Lett.* **2006**, *8*, 1953; g) H. Egami, T. Katsuki, *J. Am. Chem. Soc.* **2007**, *129*, 8940; h) F. A. Davis, Y. Zhang, H. Qiu, *Org. Lett.* **2007**, *9*, 833.

[41] For mechanistic studies concerning how water affects reactions, see: a) J. F. Blake, W. L. Jorgensen, *J. Am. Chem. Soc.* **1991**, *113*, 7430; b) J. F. Blake, D. Lim, W. L. Jorgensen, *J. Org. Chem.* **1994**, *59*, 803; c) S. Kong, J. D. Evanseck, *J. Am. Chem. Soc.* **2000**, *122*, 10418; d) J. Chandrasekhar, S. Shariffskul, W. L. Jorgensen, *J. Phys. Chem. B* **2002**, *106*, 8078; e) R. N. Butler, W. J. Cunningham, A. G. Coyne, L. A. Burke, *J. Am. Chem. Soc.* **2004**, *126*, 11923; f) Y. Jung, R. A. Marcus, *J. Am. Chem. Soc.* **2007**, *129*, 5492; g) F.-Q. Shi, X. Li, Y. Xia, L. Zhang, Z.-X. Yu, *J. Am. Chem. Soc.* **2007**, *129*, 15503.

[42] Such water-assisted proton shifts have been found in many enzymatic reactions. For a recent review, see: M. R. A. Blomberg, P. E. M. Siegbahn, *Biochim. Biophys. Acta* **2006**, *1757*, 969, and references therein.

[43] For discussions on entropy overestimation in solution, see: a) J. Hermans, L. Wang, *J. Am. Chem. Soc.* **1997**, *119*, 2707; b) L. M. Amzel, *Proteins* **1997**, *28*, 144; c) M. Strajbl, Y. Y. Sham, J. Villa, Z.-T. Chu, A. Warshel, *J. Phys. Chem. B* **2000**, *104*, 4578; d) Z.-X. Yu, K. N. Houk, *J. Am. Chem. Soc.* **2003**, *125*, 13825; e) Y. Chen, S. Ye, L. Jiao, Y. Liang, D. K. Sinha-Mahapatra, J. W. Herndon, Z.-X. Yu, *J. Am. Chem. Soc.* **2007**, *129*, 10773.

[44] The nucleophilic attack of phosphine **2** on **20** needs about 3 kcal mol^{-1} more energy than the nucleophilic attack of **2** on allenoate **1** (Figure 1), which requires an activation free energy of 26.2 kcal mol^{-1} in benzene and an activation enthalpy of 14.8 kcal mol^{-1}. This can be explained by FMO theory: the LUMO of **20** is higher than **1** by 0.18 eV.

[45] A similar water-assisted [1,3]-H shift was also found by Padwa et al. in the isomerization of the carbonyl ylide to the thermodynamically more stable azomethine ylide, see: A. Padwa, D. C. Dean, L. Zhi, *J. Am. Chem. Soc.* **1992**, *114*, 593.

[46] After many attempts, the transition state **TS10** could not be located. However, the reaction between the olefinic anion and water is expected to be very facile with a very low activation barrier.

[47] In this isotopic labeling experiment, both [1,3]- and [1,2]-hydrogen shifts are involved. According to the computational results, both of these hydrogen shifts are catalyzed by water which is supported by this experiment.

[48] a) B. M. Trost, U. Kazmaier, *J. Am. Chem. Soc.* **1992**, *114*, 7933; b) C. Guo, X. Lu, *J. Chem. Soc. Perkin Trans. 1* **1993**, 1921.

[49] After submitting this manuscript, it was reported that methanol serves as a shuttle to transfer the proton from carbon to oxygen in the Morita–Baylis–Hillman reaction, see: R. Robiette, V. K. Aggarwal, J. N. Harvey, *J. Am. Chem. Soc.* **2007**, *129*, 15513.

Received: November 1, 2007
Published online: March 20, 2008

